

Technical Addendum to the Winningsplan Groningen 2016

Production, Subsidence, Induced Earthquakes and Seismic Hazard and Risk Assessment in the Groningen Field

PART III Hazard

The report “Technical Addendum to the Winningsplan Groningen 2016 - Production, Subsidence, Induced Earthquakes and Seismic Hazard and Risk Assessment in the Groningen Field” consists of five separate documents:

Document 1	Chapters 1 to 5;	Summary and Production
Document 2	Chapter 6;	Subsidence
Document 3	Chapter 7;	Hazard
Document 4	Chapter 8;	Risk
Document 5	Chapter 9;	Damage and Appendices.

Each of these documents is also available as a *.pdf file of a size smaller than 10Mbyte, allowing sharing through e-mail.

© EP201603238413 Dit rapport is een weerslag van een voortdurend studie- en dataverzamelingsprogramma en bevat de stand der kennis van april 2016. Het copyright van dit rapport ligt bij de Nederlandse Aardolie Maatschappij B.V. Het copyright van de onderliggende studies berust bij de respectievelijke auteurs. Dit rapport of delen daaruit mogen alleen met een nadrukkelijke status-en bronvermelding worden overgenomen of gepubliceerd.

Contents

7	Hazard Assessment	4
	Hazard Metric	4
	Peak Ground Acceleration	4
	Probabilistic Hazard Assessment	6
	Seismic Event Rate and Total Seismic Moment Rate with time	6
	Ground Acceleration incorporating Local Site Effects	13
	Hazard Logic Tree	16
	Hazard Assessment	17
	Disaggregation of Seismic Hazard	23

7 Hazard Assessment

Hazard Metric

Different metrics have been proposed to describe the hazard resulting from seismic activity. Most commonly used are the peak ground velocity (PGV) and peak ground acceleration (PGA). Because PGA is a widely used metric for ground shaking intensity, it was chosen as the most appropriate hazard metric for this seismic hazard assessment. When extending the assessment to encompass risk (i.e. the response of buildings to ground shaking), spectral acceleration (SA) will be used – this takes into account the response period of the building being considered. Figure 7.1 shows the measured acceleration near the epicentre during the Huizinge earthquake of 16th August 2012. In addition to the peak PGA values, the duration of the event is also important for the seismic risk.

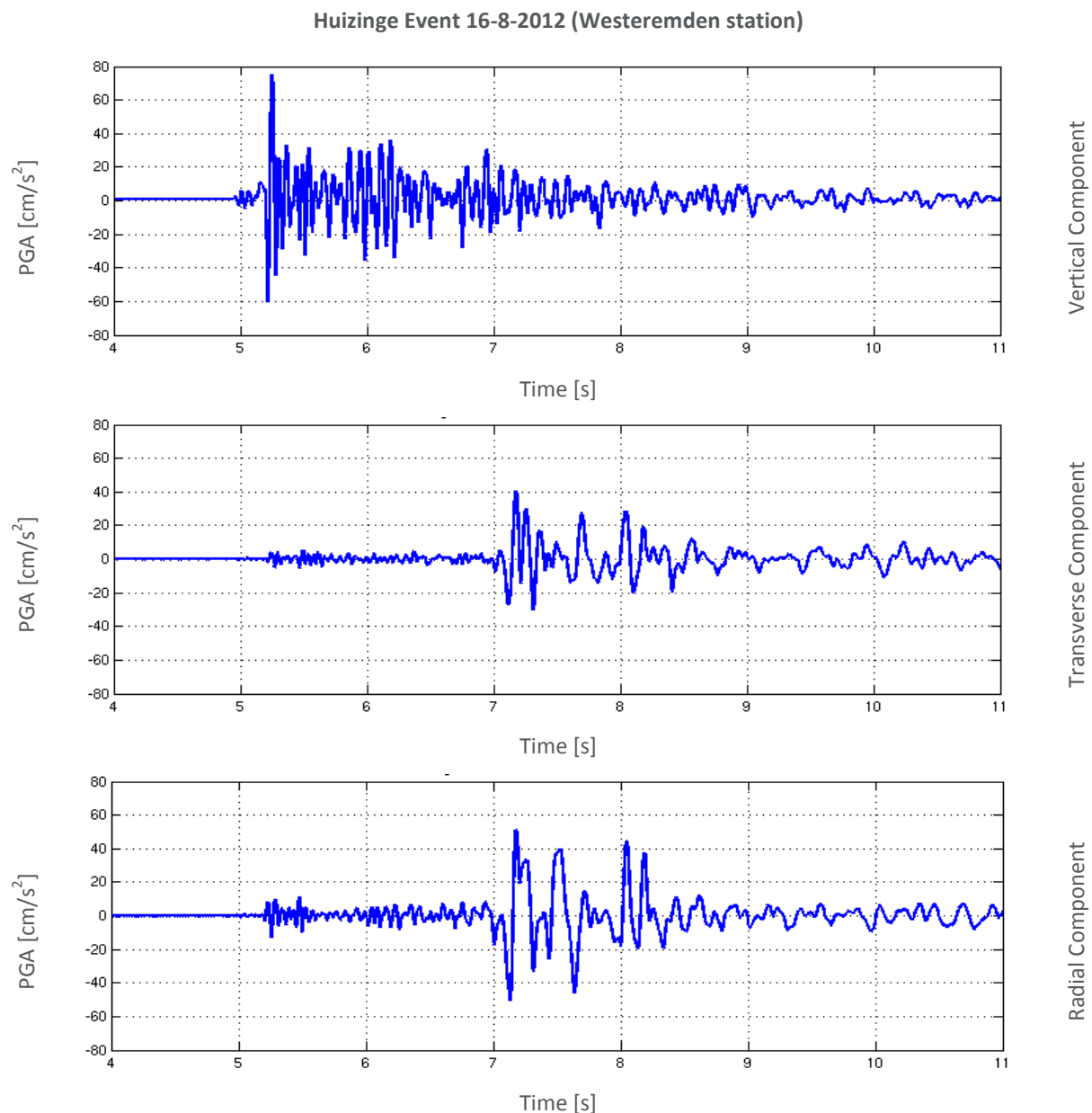


Figure 7.1 Accelerogram of the earthquake near Huizinge recorded at the 16th August 2012 by the accelerometer located near Westeremden (near the epicentre).

Peak Ground Acceleration

For the probabilistic description of the ground accelerations (PGA, or generalised to Peak Spectral Acceleration, PSA), a hazard map is used. On this map for each location the acceleration is plotted that could

occur, with a prescribed annualised probability of exceedance (exceedance level), during a prescribed analysis period. Hazard levels are shown using a gradual colour scale.

The hazard maps shown in the section were constructed according to the following procedure. Each location in the analysis area during the analysis period is subjected to ground motion accelerations resulting from induced earthquakes. At some locations, e.g. near Loppersum, the chance of exceeding a given peak ground acceleration threshold is higher than at the periphery of the field. Equally, at any one location, the chance of exceeding some value of peak ground acceleration decreases with increasing peak ground acceleration. An example of a set of hazard curves is shown for a number of locations in figure 7.2. Each declining line indicates the hazard curve for a single location in the field.

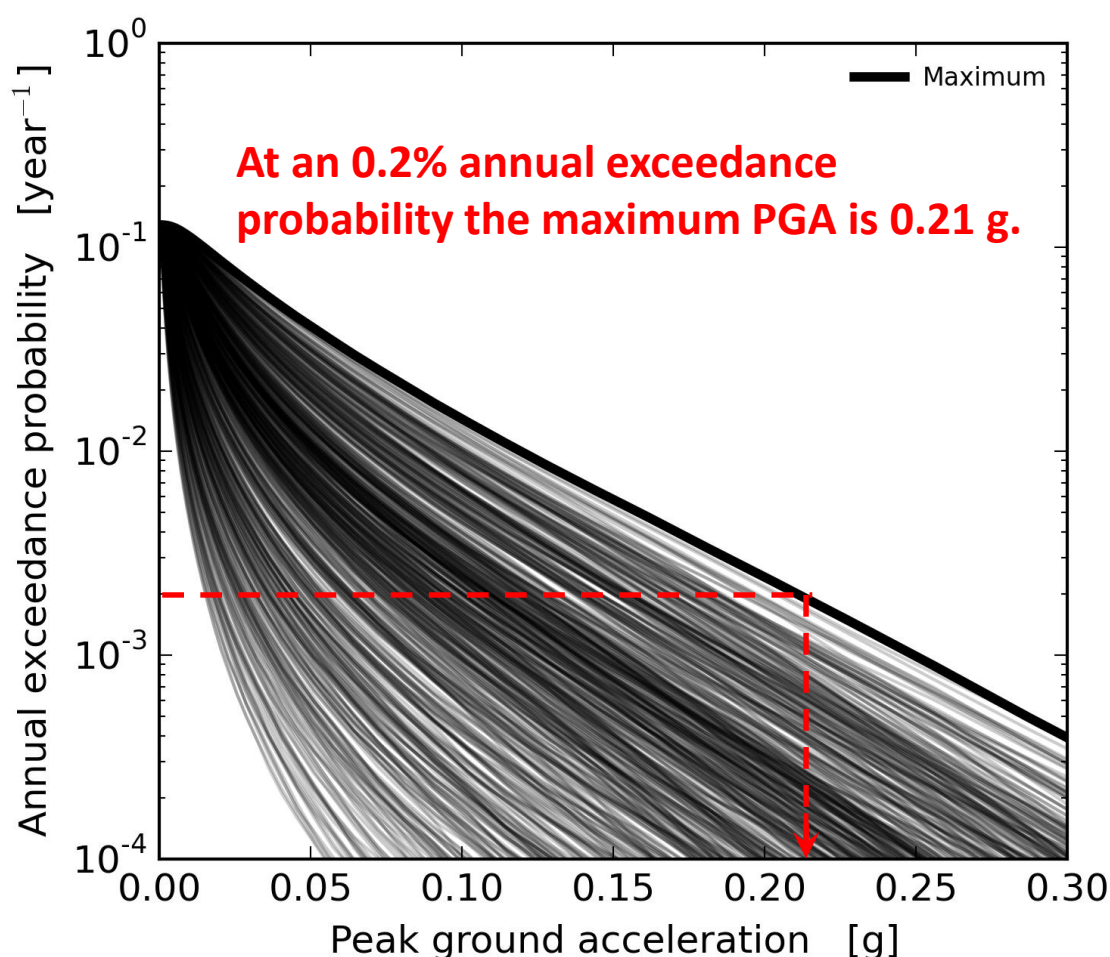


Figure 7.2 An example of a set of hazard curves showing average annual exceedance rate for peak ground acceleration at different locations in the field. Each line corresponds to a location in the field. The bold line indicates the maximum PGA anywhere within the field for a given exceedance level (bounding envelope). In this figure, the red line indicates that for an exceedance level of 0.2%/year the highest PGA in the field is 0.21g.

To prepare a hazard map, an exceedance level needs to be chosen. This is not a purely technical choice. However, inspired by Eurocode 8¹, part of the current technical standards for structural design in Europe, it has become common practice to prepare hazard maps for an exceedance level of 0.2%/year. This exceedance level is equivalent to a 475-year return period for stationary seismicity. The same exceedance level is also used by KNMI for their hazard maps. Hazard maps can be made for different production scenarios.

¹ The Eurocodes are the current technical standards for structural design in Europe, and it is now compulsory for the 28 countries in the Eurocode zone to adopt these. Eurocode 8 specifically deals with earthquake-resistant design of structures (CEN, 2006). Each country adopting Eurocode 8 must develop a National Annex to indicate how the code is implemented; the National Annex for the Netherlands is being developed. Eurocode 8 uses a standard practice to represent seismic hazard via PGA maps associated with ground motions having a 10% probability of exceedance during 50 years, equivalent to 0.2%/year for a stationary process, or a return period of 475-years.

Probabilistic Hazard Assessment

Seismic Event Rate and Total Seismic Moment Rate with time

Starting at the first step of the causal chain, from gas production via the resulting compaction, seismicity can be assessed. Seismicity is interpreted in this context as the event rate density of earthquakes larger than $M \geq 1.5$ and the frequency-magnitude distribution characterised by its slope (b-value) and upper bound (M_{\max}). This minimum earthquake magnitude of $M = 1.5$ corresponds to the minimum magnitude of an earthquake, which the installed KNMI geophone network was historically able to record reliably (independent of its location within the field boundary or time of day). Earthquakes with smaller magnitude may not always be detected, because the signal may not be distinguished from the background noise.

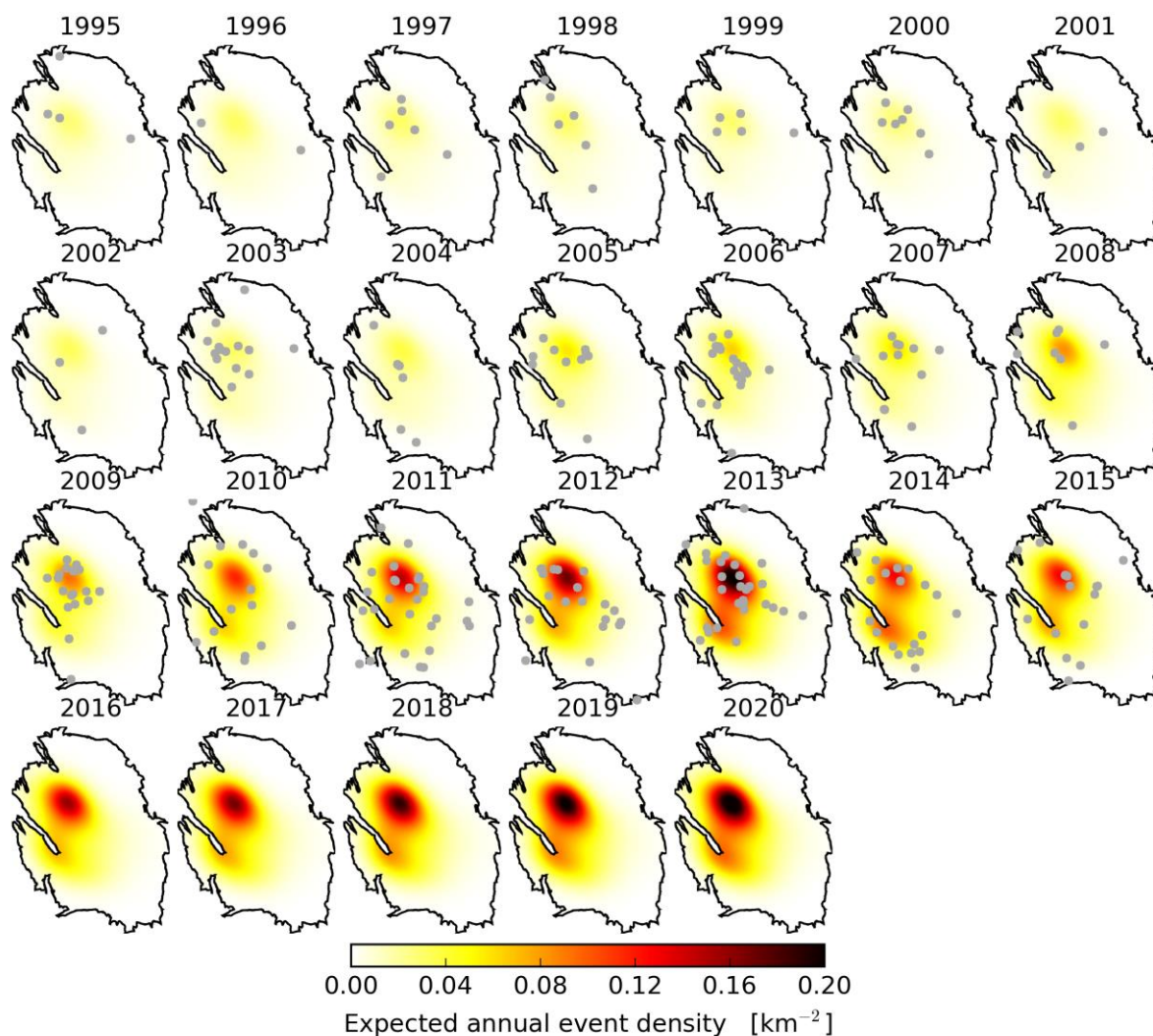


Figure 7.3 Expected annual event density maps over from 1995 to 2020 according to the seismological model. The forecast period is based on the production plan for 33 bcm/year and the linear compaction model. Grey dots denote the observed epicenters of $M \geq 1.5$ events.

Expected event density maps for the period from 2016 to 2020 for various combinations of annual production volume, distribution of production over the field and compaction model are shown in figures 7.4A, 7.4B, and 7.4C. As the event density maps through time are very similar for the linear and RTCiM compaction models, the event density used for the hazard and risk assessment in the winningsplan 2016 is based on compaction calculated using the linear compaction model.

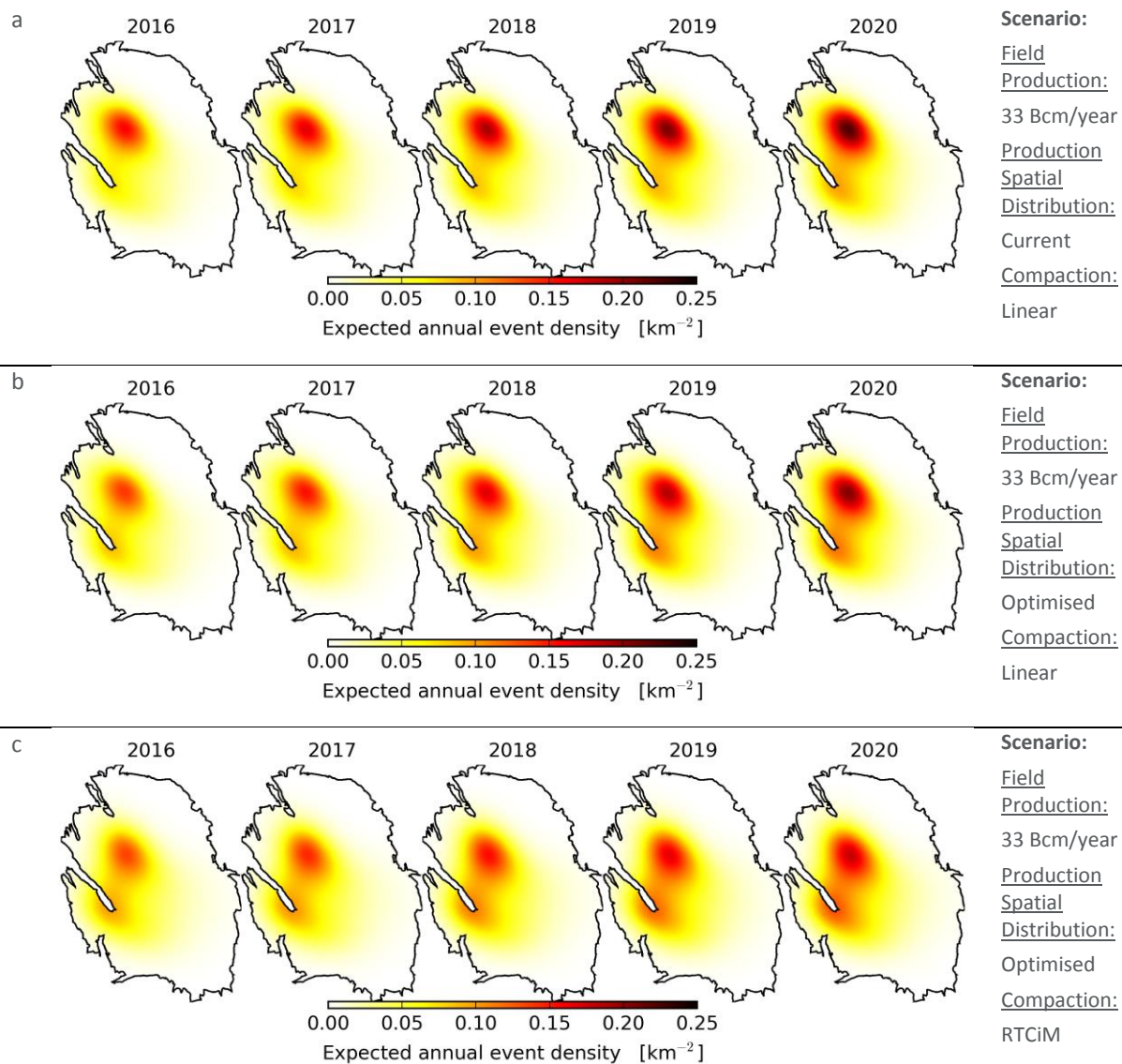


Figure 7.4A Expected annual event density maps for the 33 bcm production scenarios.

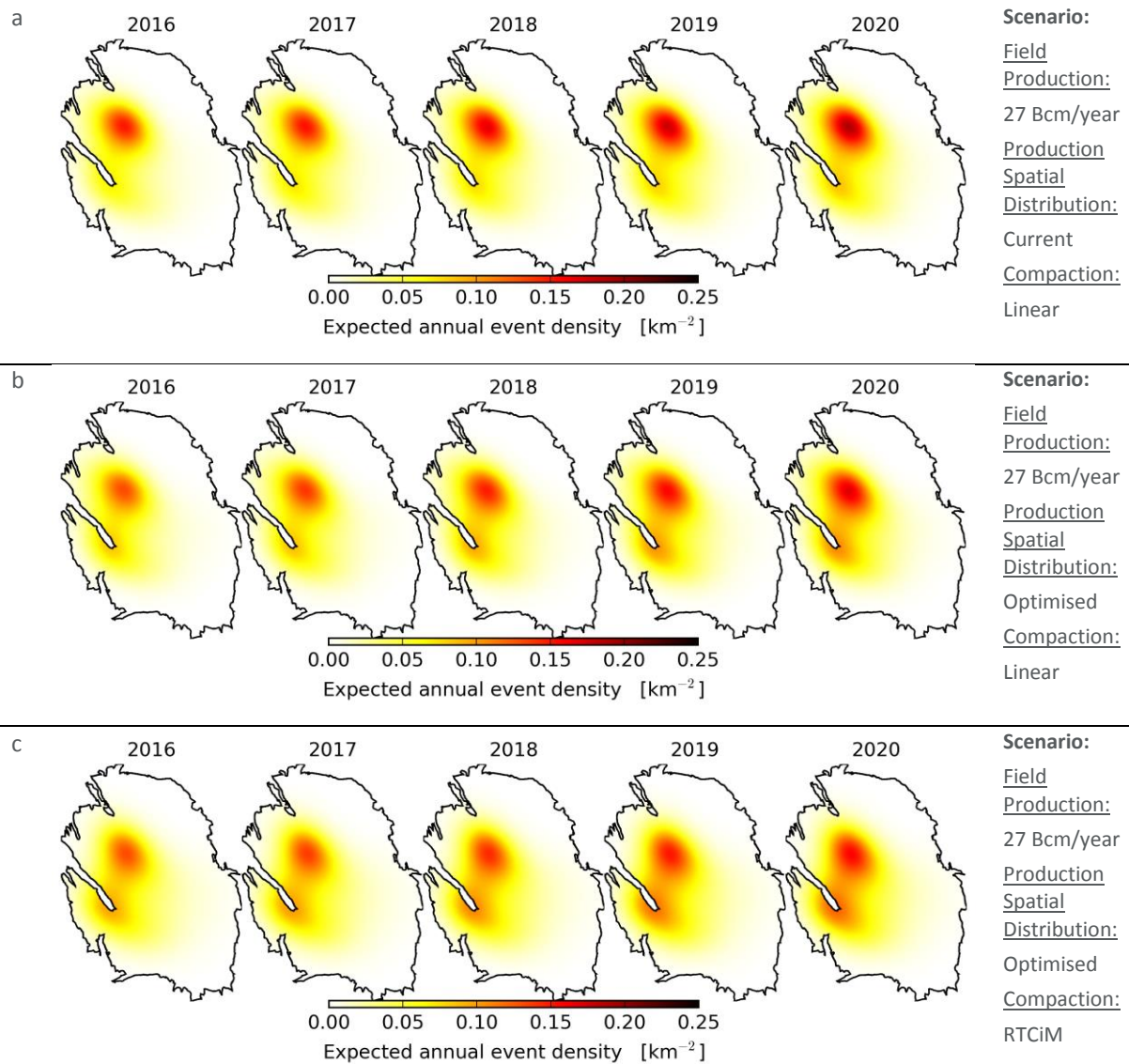


Figure 7.4B Expected annual event density maps for the 27 bcm production scenarios.

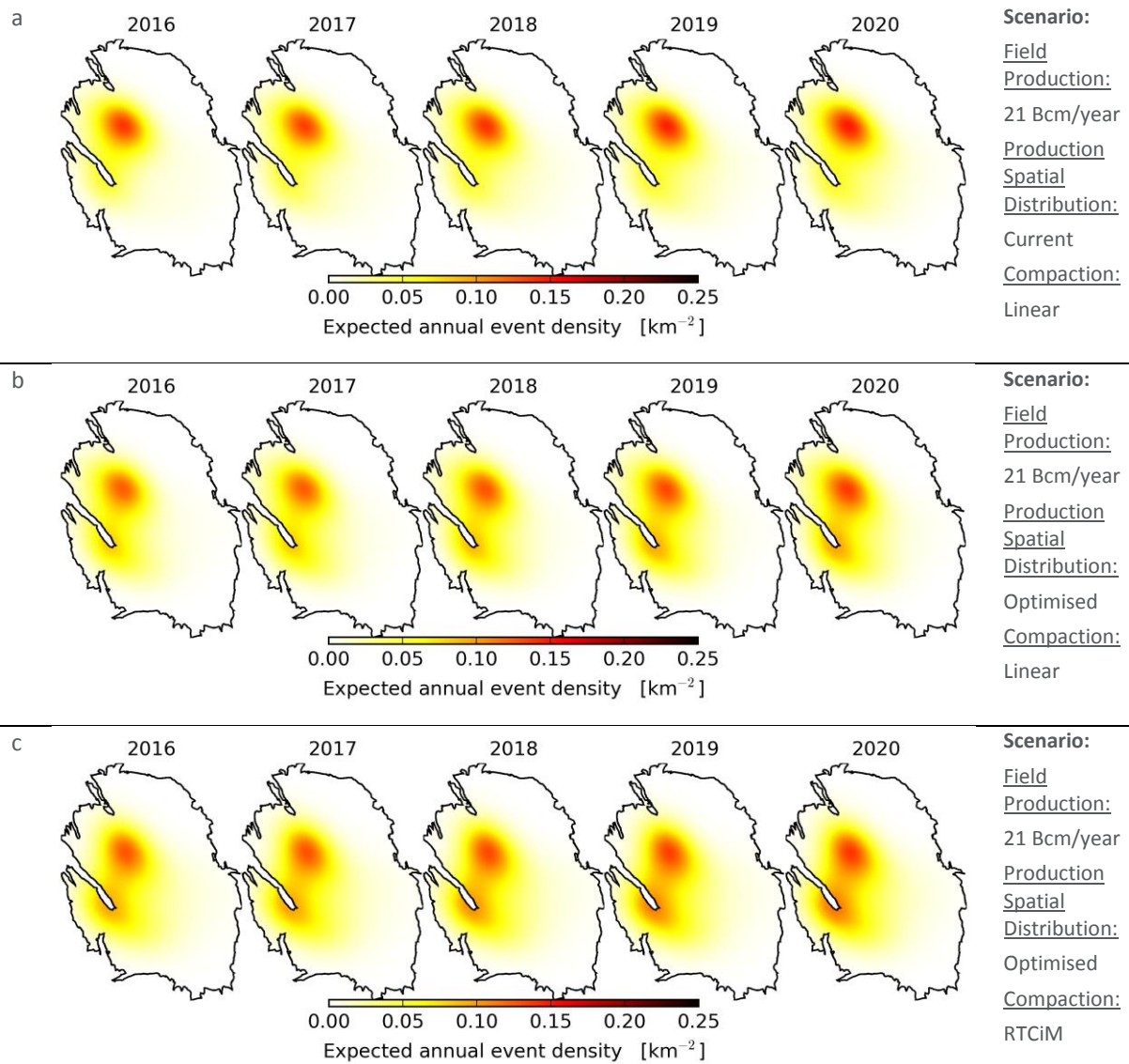


Figure 7.4C Expected annual event density maps for the 21 bcm production scenarios.

The difference maps based on the annual event density maps for these production scenarios, show the impact of the changes in annual field production (fig. 7.5) and of the distribution of the production over the field (fig. 7.6).

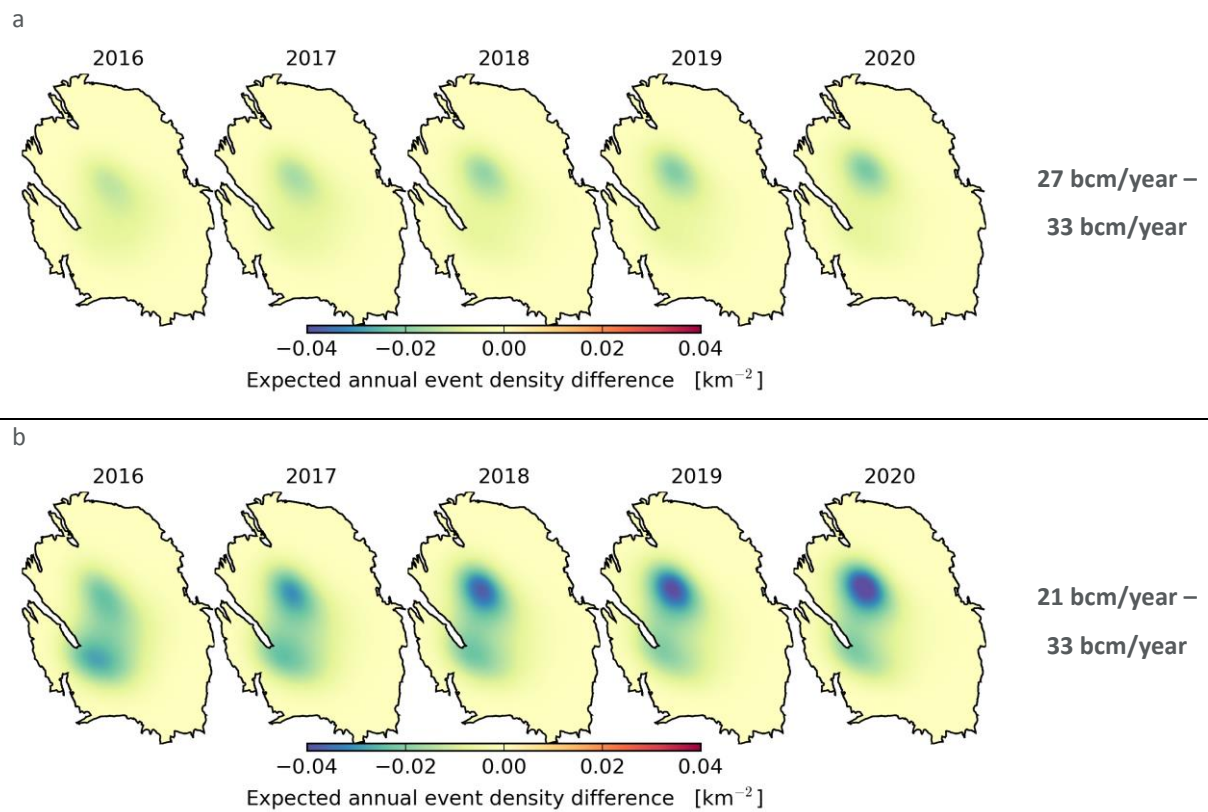


Figure 7.5 Reduction in the expected event density due to reduced gas production for the linear compaction model: (a) 27 bcm - 33 bcm, and (b) 21 bcm - 33 bcm. Please note that the variation in colour denotes a small fractional variation in density differences.

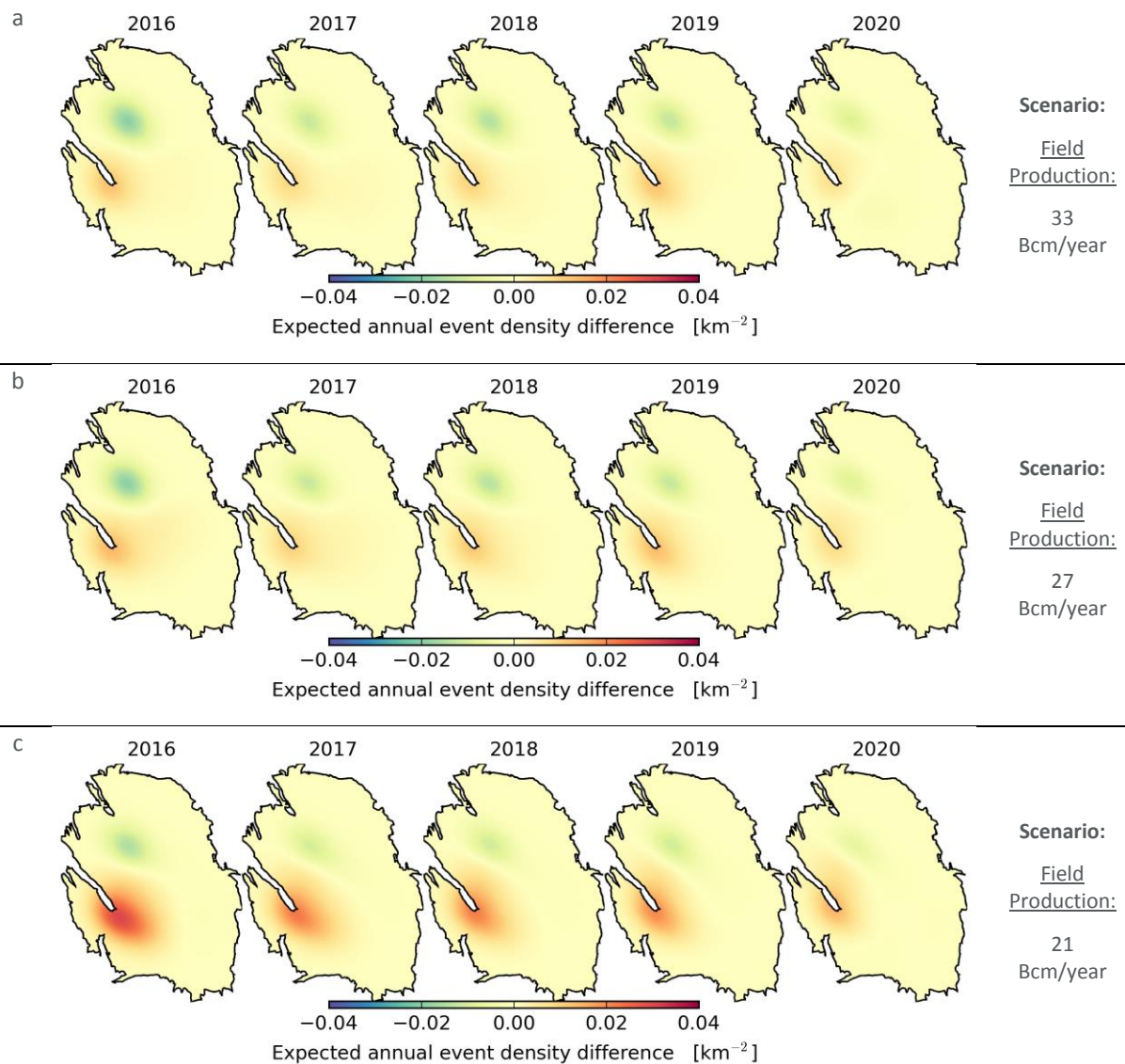


Figure 7.6 Reduction in the expected event density due to reduced gas production for the linear compaction model: (a) 33 bcm - 33(optimised) bcm, (b) 27 bcm - 27(optimised) bcm, and (c) 21 bcm - 21(optimised) bcm. Please note that the variation in colour denotes a small fractional variation in density differences.

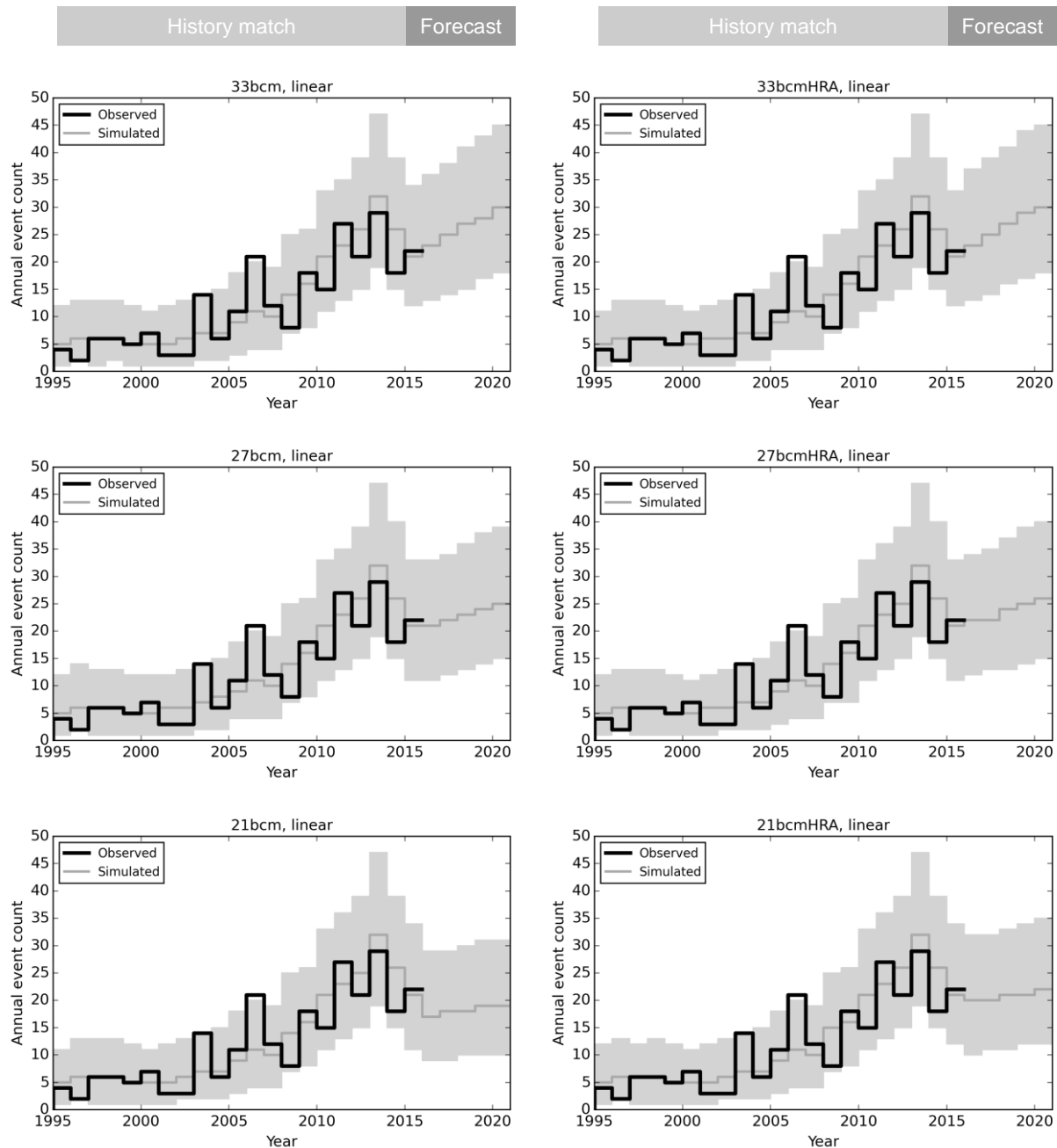


Figure 7.7 The annual number of $M \geq 1.5$ according to the seismological model with aftershocks for the different production scenarios. Simulated results are based on 10,000 independent simulations; grey lines and regions denote the expected annual event count and its 95% confidence interval respectively. These simulations are based on Monte Carlo sampling of the distribution of estimated parameter values and includes aftershocks.

Over the period from 1995 to 2015, the results of the Monte Carlo simulation and the observations for the annual event count and annual total seismic moments are shown in figure 7.7 and 7.8 respectively. The observed annual total seismic moment fluctuates around the median values of the simulated annual total seismic moments, but remains within the grey uncertainty band (the 95% confidence interval). This indicates the model is well calibrated. For the period 2016 to 2021, the forecasted annual total seismic moments and their confidence intervals are indicated. For all three production scenarios, the median annual total seismic moment is forecasted to remain in range similar to the actual observed seismic moment in the period 2012 – 2015.

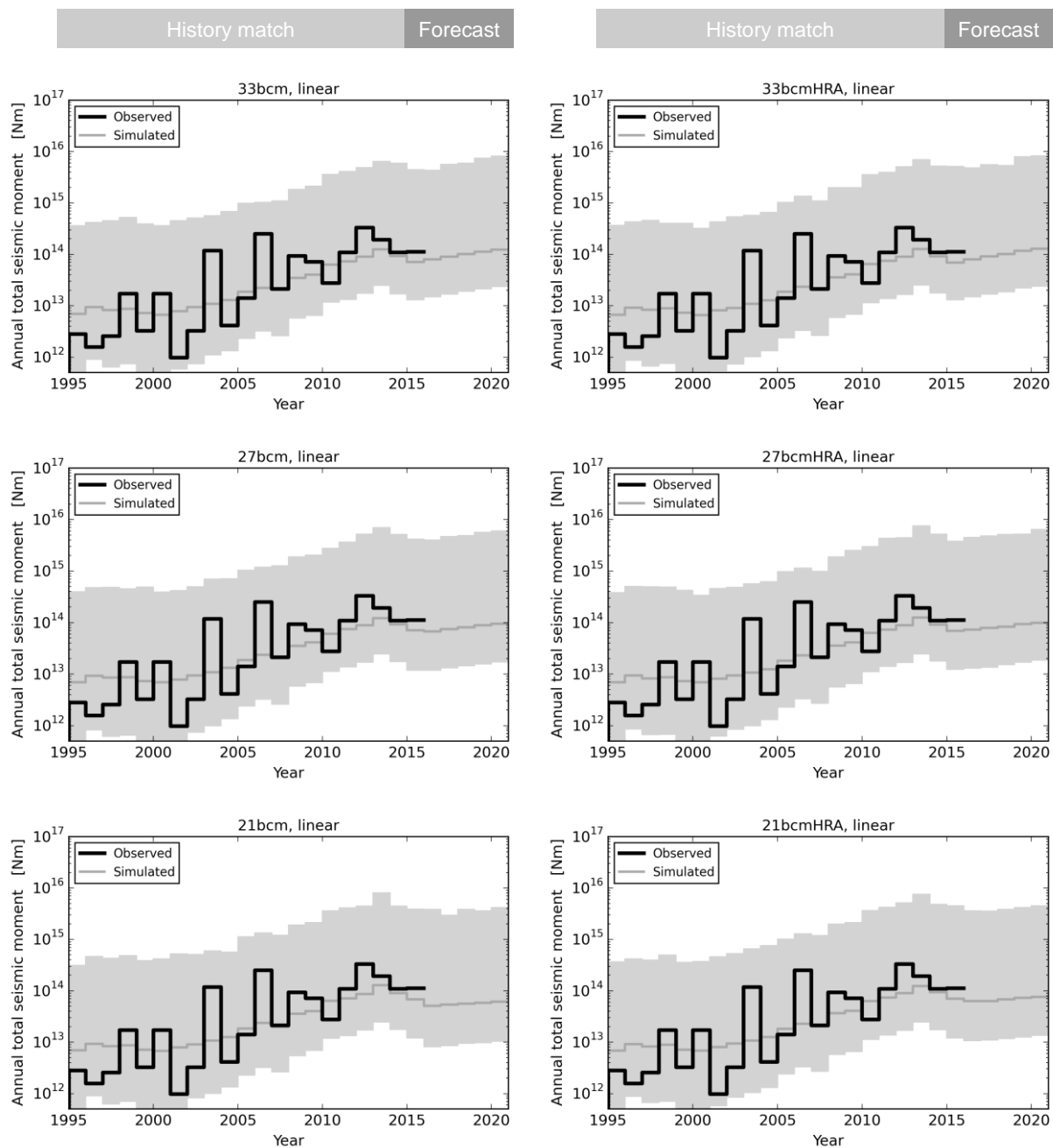


Figure 7.8 The annual total seismic moment according to the seismological model with aftershocks for the different production scenarios. Simulated results are based on 10,000 independent simulations; grey lines and regions denote the expected annual total seismic moment and its 95% confidence interval respectively. These simulations are based on Monte Carlo sampling of the distribution of estimated parameter values and includes aftershocks.

Ground Acceleration incorporating Local Site Effects

In the current hazard assessment an error in the software implementation of the model for ground motion prediction has been corrected. This was recently detected by a detailed comparison of hazard and risk results obtained from two independent software implementations and has been discussed with KNMI, TNO, SodM and SAC. As a result of this mistake in the interim update of the hazard and risk assessment of November 2015, the variability in the local site response was effectively set to its maximum value irrespective of the level of shaking expected in the underlying rock, whereas this variability should increase with the strength of

shaking. Correcting this mistake has resulted in a lower assessment of the probabilistic hazard and risk in the current Technical Addendum than in the interim update of the hazard and risk assessment of November 2015.

The effects of the local shallow subsurface and soils on ground acceleration can be incorporated by subdividing the Groningen field area in smaller areas, based on the observed variation in the dynamic site response reflecting differences in the subsurface composition. The reference rock horizon is the base of the Upper North Sea formation (NU_B), which is about 350 m below the ground surface. The motion are first predicted at this elevation, including random sampling from both the between-earthquake and within-earthquake components of variability, and then these rock motions are transferred to the ground surface via the site amplification factors.

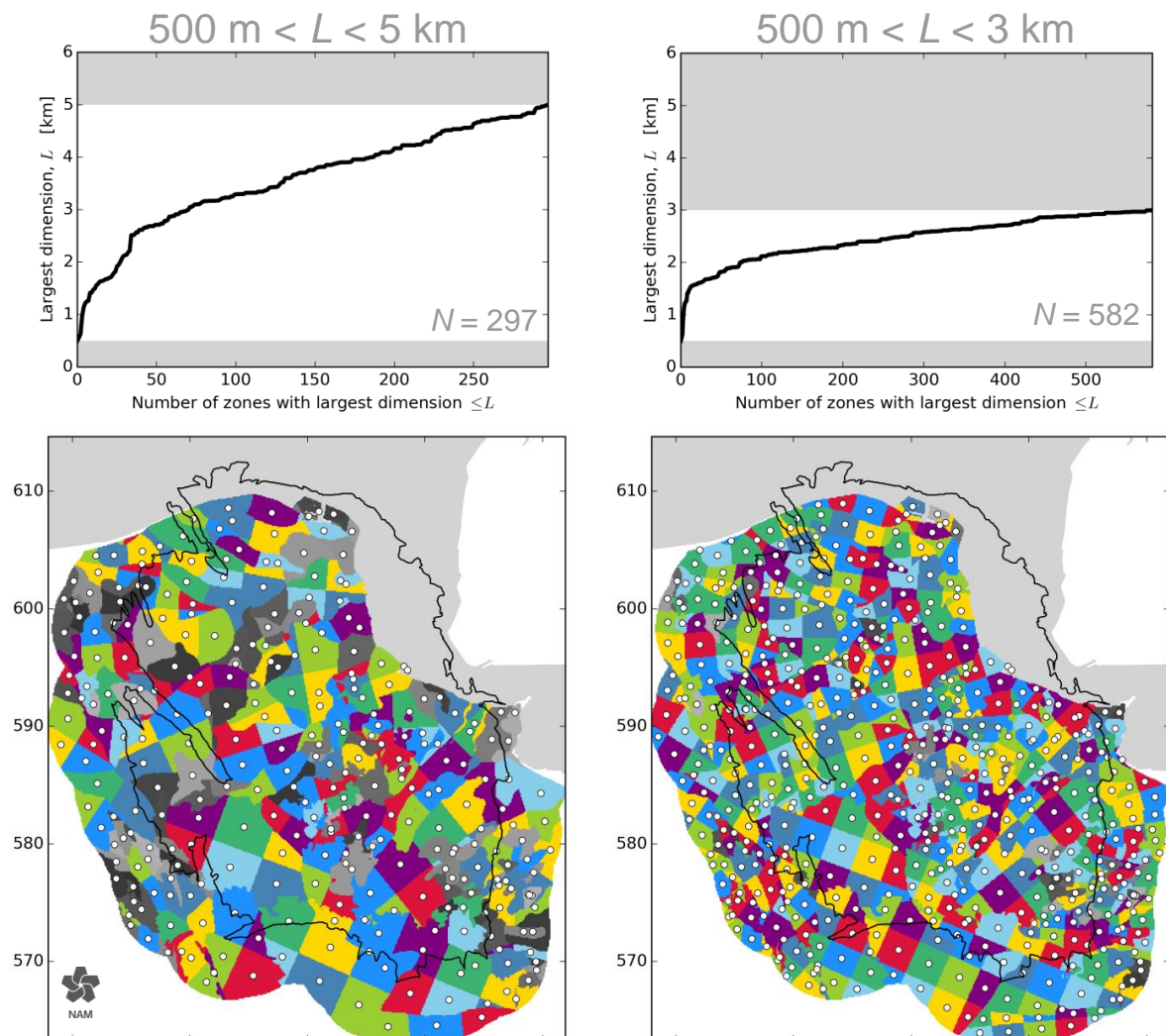


Figure 7.9 Zonation of the near-surface amplification of ground motion is represented by an irregular grid to honour the mapped geological boundaries: Left zonation with 300 zones. Right zonation with 500 zones. Note that colours do not represent any geological property but are randomly assigned to illustrate the topology of the grid.

Irregularly shaped zones were chosen to represent the complex local geological features in the shallow subsurface such as channel infills and peat areas, as realistically as possible. This causes an additional computational challenge, but leads to an improved result. Figure 7.9 shows two different zonation options. A sensitivity analysis comparing the results from using the two zonation schemes motivated the use of the zonation scheme with some 300 different soil response areas, within each which a single frequency-dependent amplification factor is applied together with a site-to-site variability term that reflects, amongst other factors, the lateral variation in site response characteristics across the zone.

Previous simulations of the acceleration caused by a single earthquake resulted in concentric PGA contours. In the current update of the hazard assessment, the effect of the soft soils is visible in the PSA map for a spectral period of 0.3s.

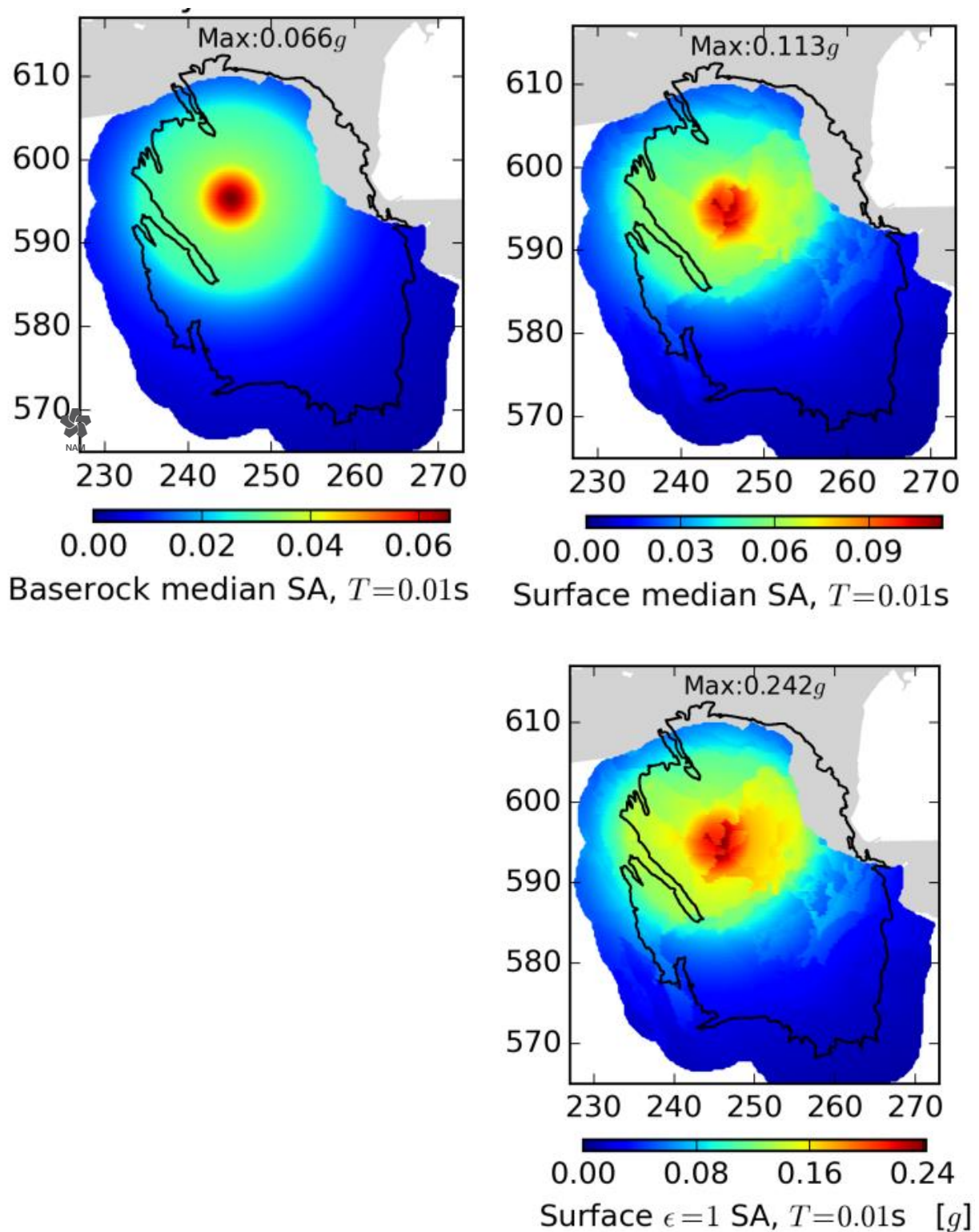


Figure 7.10 Ground motion computed on a 250m regular grid for a single $M = 5$ event at (245,595,3) km Compares base rock ($\epsilon=0$) (top left), surface ($\epsilon=0$) (top right), surface ($\epsilon=1$)(bottom right).

This effect is most clearly shown by comparing the PSA map at the base rock interface (Base Upper North Sea; NU-B) with the PGA (i.e. PSA at $T=0.01$) map at surface. Figure 7.10 shows on the left the concentric pattern of the PSA at the Base Upper North Sea at some 350 m depth. The right-hand map shows the PSA at surface with the irregular imprint of the local soils, and the highest simulated PSA away from the earthquake epicentre.

Another important feature of the site amplification factors is the fact that the site amplification factors include the non-linear behaviour of these soft soil deposits when subject to stronger levels of rock acceleration. For each zone and each response period, the site amplification factors are defined as a function of rock acceleration; as a result of the Monte Carlo approach, the site response factors are conditioned on the actual realisation of the rock motions rather than the median motions. At shorter response periods, the amplification factors decrease with increasing rock acceleration due to the softening of the soil and the increase damping associated with larger shear strains; at long response periods, the pattern is reversed as a result of the elongation of the fundamental site period.

Hazard Logic Tree

In preparing the hazard maps, the uncertainty in the most important parameters has been incorporated by using scenarios. These scenarios are captured in the logic tree. The logic tree for the hazard is shown in figure 7.11. These scenarios are combined using the weights in the logic tree to provide the mean hazard map. The scenarios for maximum magnitude have equal weights as was also used in the hazard assessment of November 2015. At the workshop on maximum magnitude (held March 2016), a panel of internationally recognised experts was asked to provide their assessment of the distribution of the maximum magnitude. Once their assessment is available, this part of the logic tree will be updated accordingly in future hazard and risk updates.

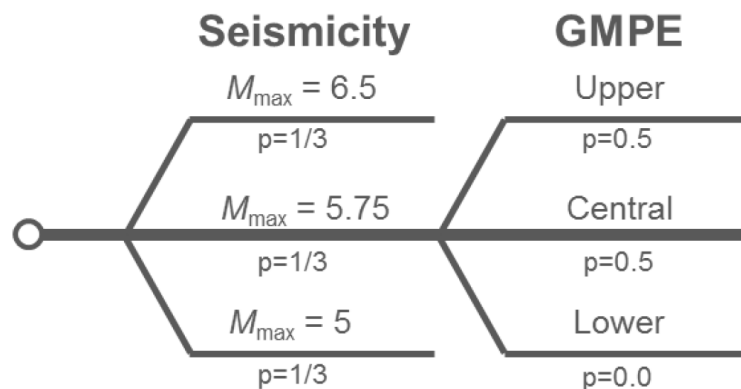


Figure 7.11 Logic tree used for assessing seismic hazard.

The weights for the different GMPE branches on the logic tree are based on the guidance by SodM in the expectation letter (verwachtingenbrief²) (Fig. 7.12). The lowest branch was removed; rather than re-distribute the weights so that the relative confidence in the other two branches is maintained, the SodM expectation specified equal weighting on the central and upper branches.

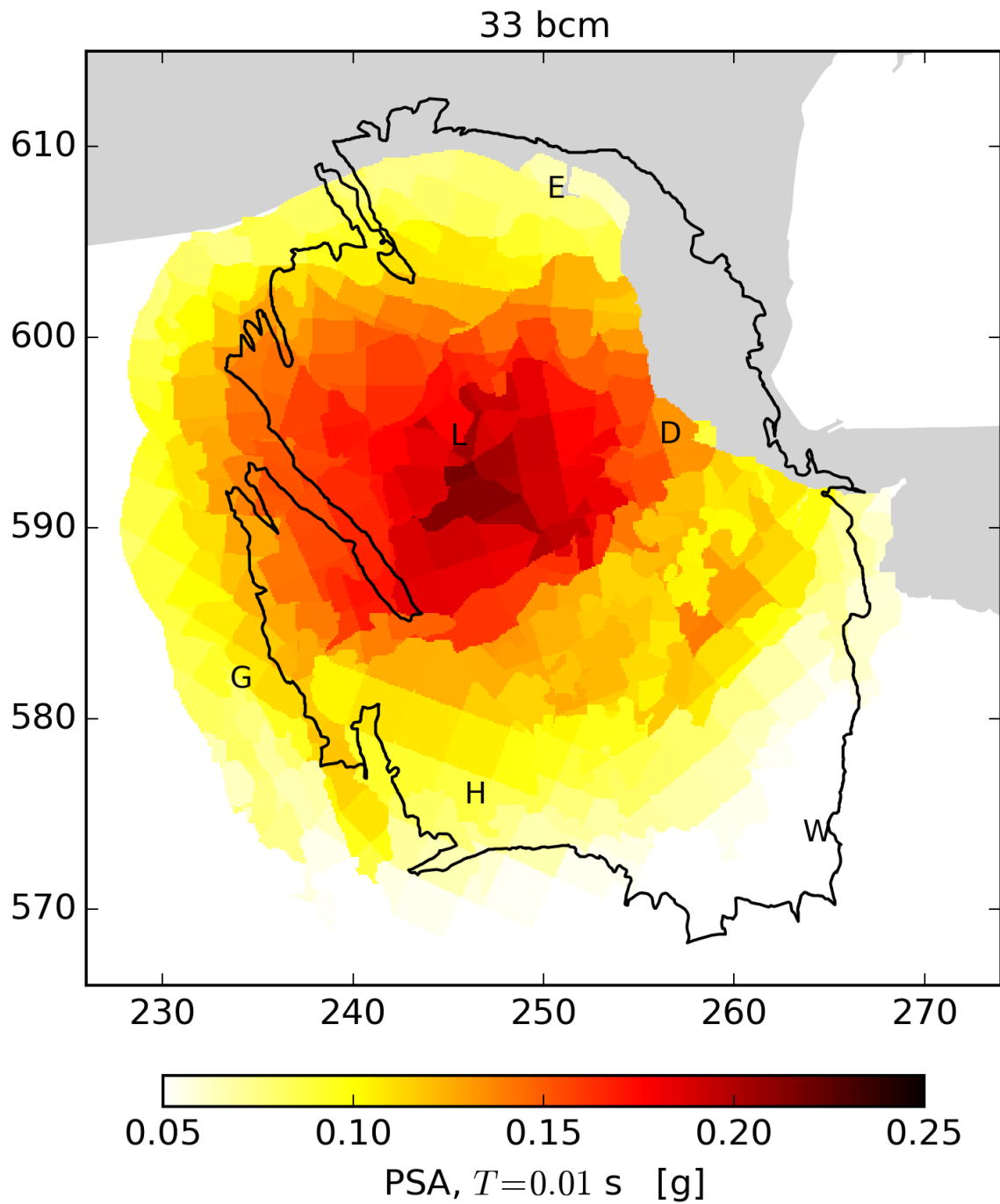
² EZ, Verwachtingenbrief winningsplan Groningenveld 2016, DGETM-EO / 16021708, 15 February 2016 – See Appendix B of the Winningsplan 2016.

7. NAM verwerkt in de risicoanalyse rekening het commentaar van de Scientific Advisory Committee (SAC) en de onafhankelijke deskundigen die SodM heeft ingeschakeld (zie referenties 5.2, 5.3 en 5.4 bij het advies van SodM over het Seismisch Risico Groningenveld van december 2015). Dit commentaar geeft aan dat de GMPE-relatie, de vertaling van de bewegingen bij de bron van de beving naar het aardoppervlak, voor sterkere (nog niet waargenomen) bevingen de grondversnellingen mogelijk is onderschat. Er wordt een risico inschatting (Individueel en Maatschappelijk risico) verwacht op basis van een beslisboom waarin de onderste (lage) GMPE tak is weggelaten en de overige twee takken eenzelfde gewicht toegekend krijgen.

Figure 7.12 Guidance from SodM in the expectation letter (verwachtingenbrief).

Hazard Assessment

The impact of lateral heterogeneity in composition of the shallow subsurface in the hazard map is less apparent than in the acceleration response at surface to a single earthquake. This is because the mean hazard map combines the effects of all forecast earthquakes in the evaluation period (2016-2012) which span a wide range of locations, magnitudes and all branches of the logic tree. The hazard map for the scenario of an annual field production of 33 Bcm/year and the current offtake distribution is shown in figure 7.13.



Max PGA = 0.21g
2016/1 – 2021/1

Figure 7.13 PGA hazard maps Period: 2016 – 2021, Production: 33 bcm/year, Compaction: Inversion, Activity Rate Model: Version V2, $3.5 \leq M \leq 6.5$, Metric: $0.2\% \text{ year}^{-1}$ chance of exceedance (10% chance in 50 years). Mean hazard from logic tree.

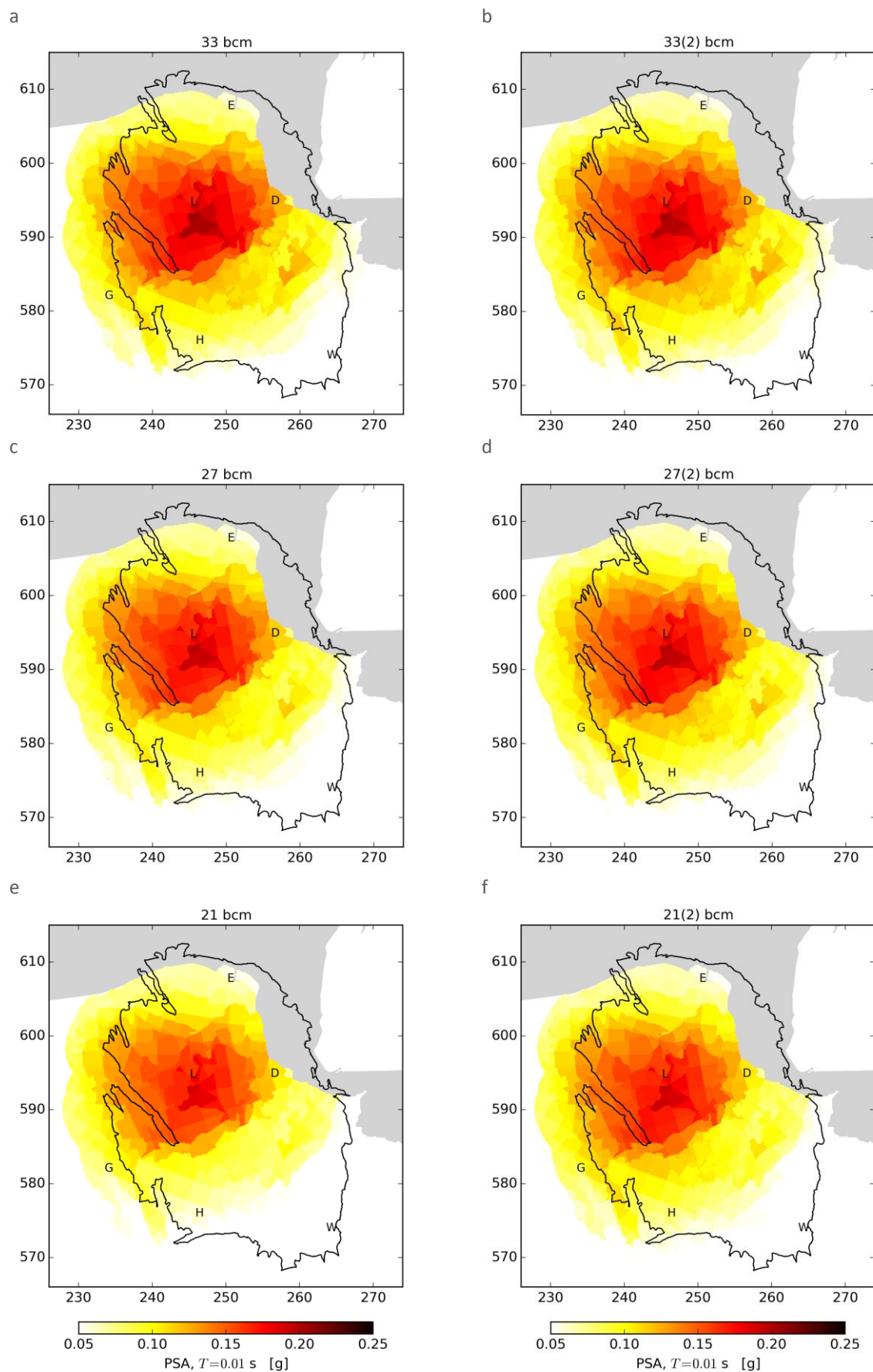


Figure 8.14 Mean PGA hazard maps with an average 0.2% annual chance of exceedance (1 in 475 years) from 1/1/2016 to 1/1/2017 given the V2 linear compaction model and 6 production scenarios. Maximum values of the mean PGA hazard are: (a) 0.206g, (b) 0.204g, (c) 0.200g, (d) 0.199g (e) 0.191g, (f) 0.194g.

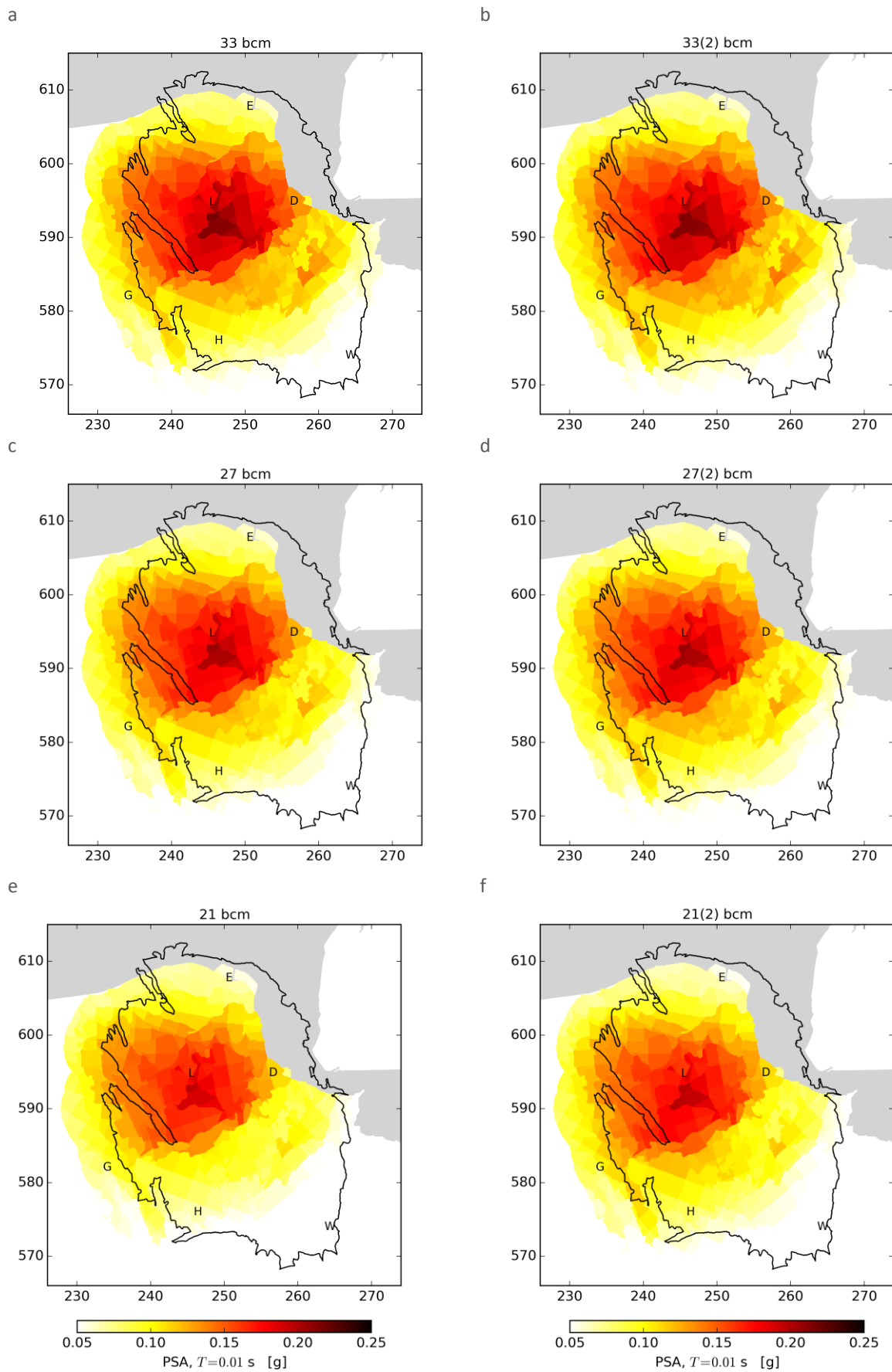


Figure 7.15 As previous figure, except for the 5-year period 2016-2021. Maximum values of the mean PGA hazard are: (a) 0.218g, (b) 0.215g, (c) 0.208g, (d) 0.207g (e) 0.197g, (f) 0.198g.

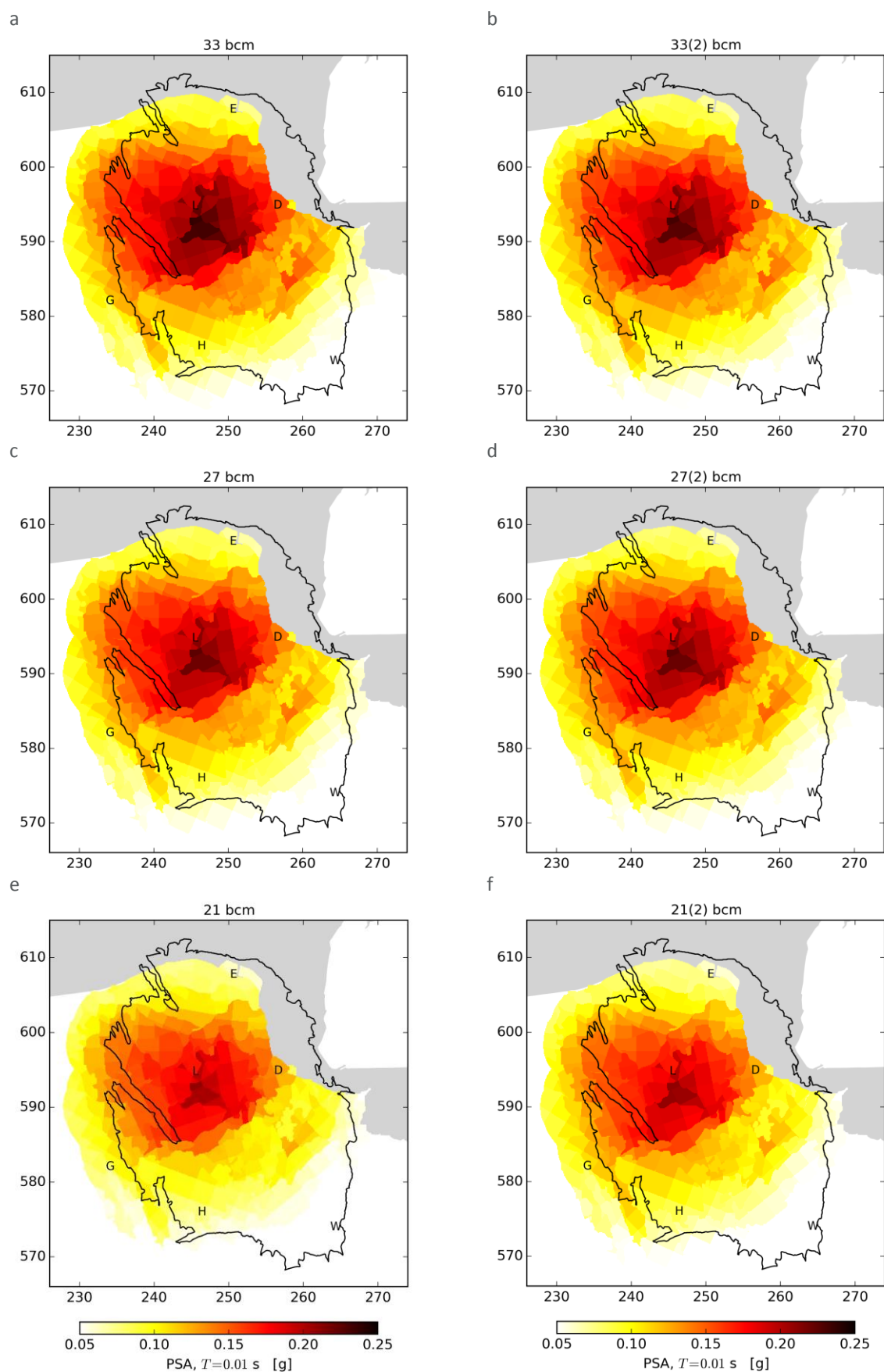


Figure 8.16 As previous figure, except for the next 5-year period 2021-2026. Maximum values of the mean PGA hazard are: (a) 0.238g, (b) 0.232g, (c) 0.226g, (d) 0.227g, (e) 0.210g, (f) 0.210g.

Disaggregation of Seismic Hazard

The question which earthquakes have most impact on the hazard assessment was studied through a disaggregation of the hazard. Two disaggregations are shown; one for the hazard in the Loppersum area (Fig. 7.17) and one for the city of Groningen (Fig. 7.18).

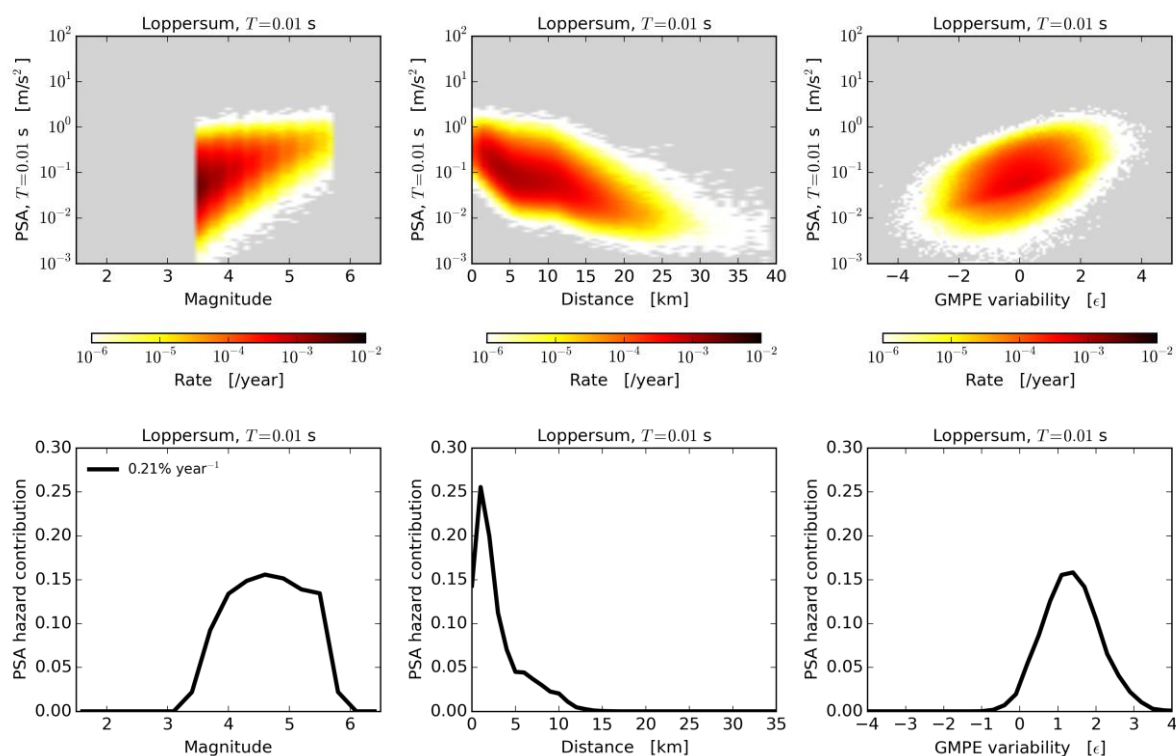


Figure 8.17 (a) Occurrence rates for peak spectral acceleration at 0.01 s as a function of magnitude, distance, and GMPE epsilon, ϵ , for a single surface location directly above the region of maximum reservoir compaction. Grey denotes no occurrence in any of the simulations. (b) The fractional contribution to the ground motion with a 0.2% annual probability of exceedance from January 2016 to January 2021.

The disaggregation of the hazard for the Loppersum area shows that the largest contribution to the hazard is from earthquakes within the Loppersum area (small distance of less than 5 km away with a magnitude ranging from 4 to 5). In contrast the largest contribution to the hazard in the Groningen city is from earthquakes with an epicenter approximately 10 km away from the city (towards the Loppersum area). To cause significant ground acceleration in the city of Groningen, these earthquakes located further away require a larger magnitude or GMPE epsilon to cause similar ground motions.

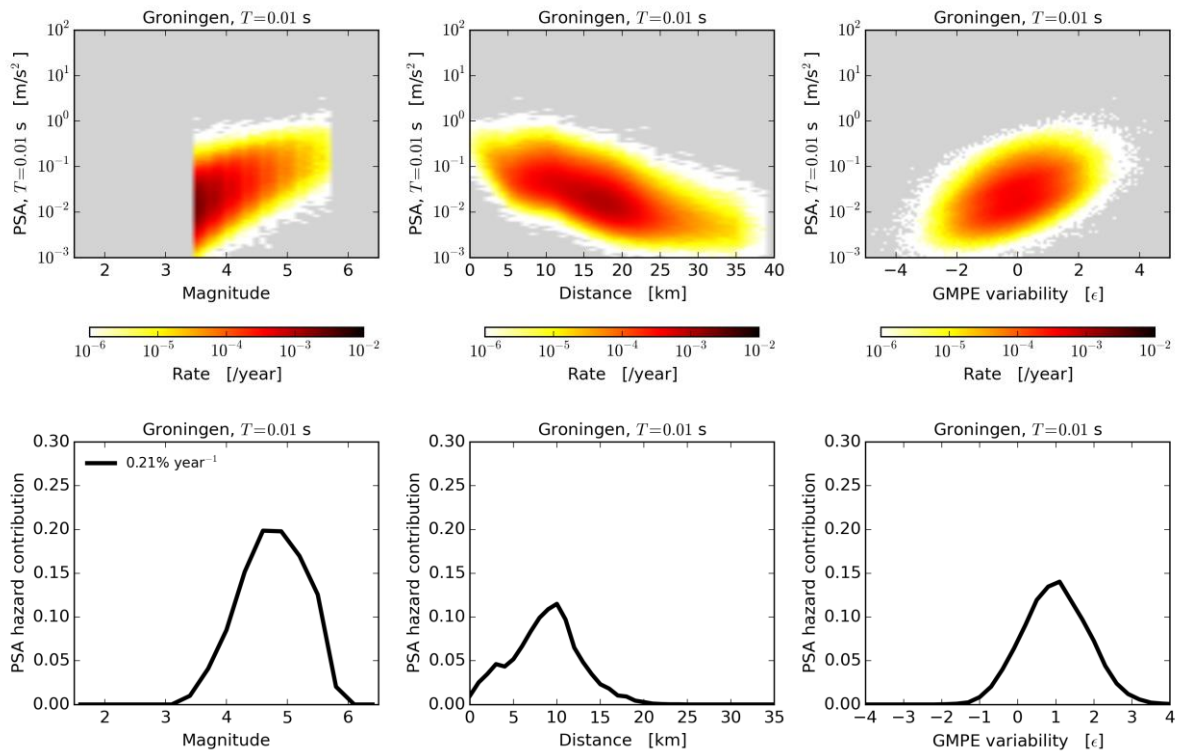


Figure 8.18 As previous figure, except for a surface location in the center of Groningen city.

Sites with poor site response ($\epsilon \geq 0$) contribute most to the hazard for the Loppersum area and the city of Groningen, with the largest contribution for $\epsilon=1$.

Insight into the disaggregation for the Groningen area is shown in figure 8.19. It confirms that the largest contribution to the hazard in the Loppersum area comes from earthquakes with a magnitude 4 to 5. Away from the Loppersum area, in Groningen stad, Delfzijl and Eemshaven, the largest contribution comes from larger earthquakes.

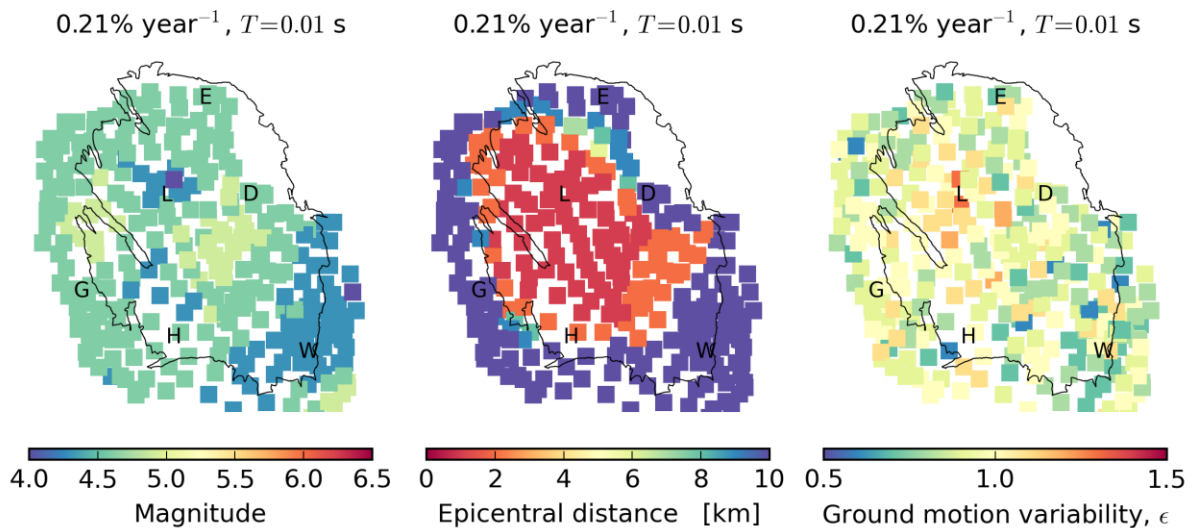


Figure 8.19 Maps of the magnitude, epicentral distance, GMPE epsilon that contribute most to the PGA hazard with a 0.2% annual chance of exceedance at that location.

